

# Inactivation of HIF-prolyl 4-hydroxylases 1, 2 and 3 in NG2-expressing cells induces HIF2-mediated neurovascular expansion independent of erythropoietin

Andrés A. Urrutia<sup>1,2</sup>  | Nan Guan<sup>1,3</sup>  | Claudia Mesa-Ciller<sup>2</sup> | Aqeela Afzal<sup>4</sup> | Olena Davidoff<sup>1</sup> | Volker H. Haase<sup>1,5,6</sup> 

<sup>1</sup>Department of Medicine, Vanderbilt University School of Medicine, Nashville, TN, USA

<sup>2</sup>Unidad de Investigación Hospital de Santa Cristina, Instituto de Investigación del Hospital Universitario La Princesa, Universidad Autónoma de Madrid, Madrid, Spain

<sup>3</sup>Division of Nephrology, Huashan Hospital and Nephrology Research Institute, Fudan University, Shanghai, China

<sup>4</sup>Department of Neurosurgery, Vanderbilt University School of Medicine, Nashville, TN, USA

<sup>5</sup>Division of Integrative Physiology, Department of Medical Cell Biology, Uppsala Universitet, Uppsala, Sweden

<sup>6</sup>Department of Molecular Physiology and Biophysics and Program in Cancer Biology, Vanderbilt University School of Medicine, Nashville, TN, USA

## Correspondence

Andrés A. Urrutia, Unidad de Investigación Hospital de Santa Cristina, Instituto de Investigación del Hospital Universitario La Princesa, Calle Maestro Vives, 2, edificio b 5° floor, 28009 Madrid, Spain.  
Email: andres.urrutia@uam.es

Volker H. Haase, Department of Medicine, Vanderbilt University Medical Center, MCN C-3119A, 1161 21st Avenue So., Nashville, TN 37232-2372, USA.  
Email: volkerhhaase@gmail.com

## Funding information

Comunidad de Madrid and Universidad Autónoma de Madrid, Grant/Award Number: S11/PJI/2019-00399

## Abstract

**Aim:** NG2 cells in the brain are comprised of pericytes and NG2 glia and play an important role in the execution of cerebral hypoxia responses, including the induction of erythropoietin (EPO) in pericytes. Oxygen-dependent angiogenic responses are regulated by hypoxia-inducible factor (HIF), the activity of which is controlled by prolyl 4-hydroxylase domain (PHD) dioxygenases and the von Hippel-Lindau (VHL) tumour suppressor. However, the role of NG2 cells in HIF-regulated cerebral vascular homeostasis is incompletely understood.

**Methods:** To examine the HIF/PHD/VHL axis in neurovascular homeostasis, we used a Cre-loxP-based genetic approach in mice and targeted *Vhl*, *Epo*, *Phd1*, *Phd2*, *Phd3* and *Hif2a* in NG2 cells. Cerebral vasculature was assessed by immunofluorescence, RNA in situ hybridization, gene and protein expression analysis, gel zymography and in situ zymography.

**Results:** *Vhl* inactivation led to a significant increase in angiogenic gene and *Epo* expression. This was associated with EPO-independent expansion of capillary networks in cortex, striatum and hypothalamus, as well as pericyte proliferation. A comparable phenotype resulted from the combined inactivation of *Phd2* and *Phd3*, but not from *Phd2* inactivation alone. Concomitant PHD1 function loss led to further expansion of the neurovasculature. Genetic inactivation of *Hif2a* in *Phd1/Phd2/Phd3* triple mutant mice resulted in normal cerebral vasculature.

See editorial article: Rosenberger C., and Fahling M. 2021. A triple sense of oxygen promotes neurovascular angiogenesis in NG2-derived cells. *Acta Physiol.* 231. e13578.

This is an open access article under the terms of the Creative Commons Attribution-NonCommercial-NoDerivs License, which permits use and distribution in any medium, provided the original work is properly cited, the use is non-commercial and no modifications or adaptations are made.

© 2020 The Authors. *Acta Physiologica* published by John Wiley & Sons Ltd on behalf of Scandinavian Physiological Society

**Conclusion:** Our studies establish (a) that HIF2 activation in NG2 cells promotes neurovascular expansion and remodelling independently of EPO, (b) that HIF2 activity in NG2 cells is co-controlled by PHD2 and PHD3 and (c) that PHD1 modulates HIF2 transcriptional responses when PHD2 and PHD3 are inactive.

#### KEYWORDS

angiogenesis, brain, erythropoietin, HIF, pericytes, prolyl 4-hydroxylase domain

## 1 | INTRODUCTION

Although the human brain accounts for only ~2% of body weight, it consumes approximately 20% of the body's oxygen and glucose-derived energy.<sup>1</sup> When oxygen levels fall below normal range, hyperaemia coupled with redistribution of blood flow occurs immediately, thereby increasing cerebral oxygenation.<sup>2,3</sup> If the supply of oxygen remains insufficient, additional adaptive responses come into play to avert the detrimental effects of hypoxia on the brain. In this case, cells activate transcriptional and metabolic responses that are regulated by the hypoxia-inducible factor (HIF) pathway.<sup>4-6</sup> The activity of HIF transcription factors, which consist of an oxygen-regulated  $\alpha$ -subunit (either HIF1 $\alpha$ , HIF2 $\alpha$  or HIF3 $\alpha$ ) and a constitutively expressed  $\beta$ -subunit, is controlled by prolyl 4-hydroxylase domain dioxygenases PHD1, PHD2 and PHD3. PHD2 is the main dioxygenase that controls HIF activity under normoxia, as PHD2 inhibition alone is sufficient for HIF activation in many cell types.<sup>6-8</sup> HIF-PHD dioxygenases act as cellular oxygen sensors and hydroxylate specific proline residues within the HIF $\alpha$  subunit in an oxygen- and iron-dependent manner. Under normoxia, prolyl 4-hydroxylation of HIF $\alpha$  leads to its proteasomal degradation via ubiquitylation by the von Hippel-Lindau (VHL)-E3 ubiquitin ligase complex. Under hypoxia, proline 4-hydroxylation and thus HIF $\alpha$  degradation are impaired resulting in cellular HIF $\alpha$  accumulation and the formation of HIF $\alpha$ / $\beta$  heterodimers in the nucleus. This increases the expression of genes involved in the regulation of multiple biological processes such as vasculogenesis and angiogenesis, energy metabolism and erythropoiesis.<sup>4,5</sup>

In the brain, chronically low oxygen levels promote vascular remodelling through the induction of various pleiotropic and angiogenic factors including erythropoietin (EPO) and vascular endothelial growth factor A (VEGFA), which increase perfusion and delivery of oxygen to the brain parenchyma.<sup>9-14</sup> Although hypoxia-induced neurovascular angiogenesis and remodelling is a well-recognized phenomenon in neuropathology, the cell types and molecular pathways involved in this response are not well characterized.

NG2 cells play an important role in neurovascular homeostasis and consist of pericytes and NG2 glia, a subpopulation of glia that give rise to myelinating oligodendrocytes.<sup>15-17</sup> While pericytes represent an essential cellular component of

the cerebral vasculature,<sup>18</sup> NG2 glia have also been shown to contribute to neurovascular homeostasis.<sup>19</sup> Pericytes stabilize capillaries, contribute to vascular growth and are involved in blood brain barrier formation and maintenance.<sup>20</sup> They furthermore control capillary diameter and cerebral blood flow, and process toxic metabolites.<sup>17,21-23</sup> Pericytes represent a heterogeneous cell population that can be identified by certain molecular markers such as platelet-derived growth factor receptor  $\beta$  (PDGFRB) and neural/glial antigen 2 (NG2), which is encoded by the *chondroitin sulphate proteoglycan 4 (Cspg4)* gene.<sup>20</sup> NG2 is a 300-kDa single-membrane spanning chondroitin sulphate proteoglycan, which is expressed by all brain pericytes and by NG2 glia, and acts as a coreceptor for platelet-derived growth factor (PDGF).<sup>24-26</sup>

Although vascular dysfunction has been shown to worsen brain hypoxia, little is known about the role of NG2 cells in cerebral hypoxia responses.<sup>15,23,27,28</sup> To better understand the role of HIF in neurovascular homeostasis, we conditionally inactivated *Vhl*, *Phd1*, *Phd2*, *Phd3* and *Hif2a* in NG2 cells taking advantage of *Ng2-cre* transgenic mice.<sup>25</sup> We found that *Vhl* gene deletion, which results in robust HIF activation, increased capillary density in cortex, striatum and hypothalamus, pericyte proliferation and led to transcriptional and phenotypic changes consistent with vascular remodelling. These changes occurred in an EPO-independent manner. A comparable phenotype was observed when *Phd2* and *Phd3* were inactivated together, whereas *Phd2* inactivation alone did not induce a vascular phenotype. Concomitant *Phd1* inactivation in *Phd2*<sup>-/-</sup> *Phd3*<sup>-/-</sup> NG2 cells further enhanced HIF2-dependent neurovascular expansion.

In summary, our studies suggest that NG2 cells play a key role in neurovascular vasculogenesis and angiogenesis that is EPO-independent and identify distinct roles for individual HIF-PHDs in the regulation of HIF2-dependent transcriptional responses.

## 2 | RESULTS

### 2.1 | *Vhl* deletion in NG2 cells expands and remodels neurovasculature

To examine the neurovascular consequences of HIF activation in NG2 cells, we targeted the VHL tumour suppressor.

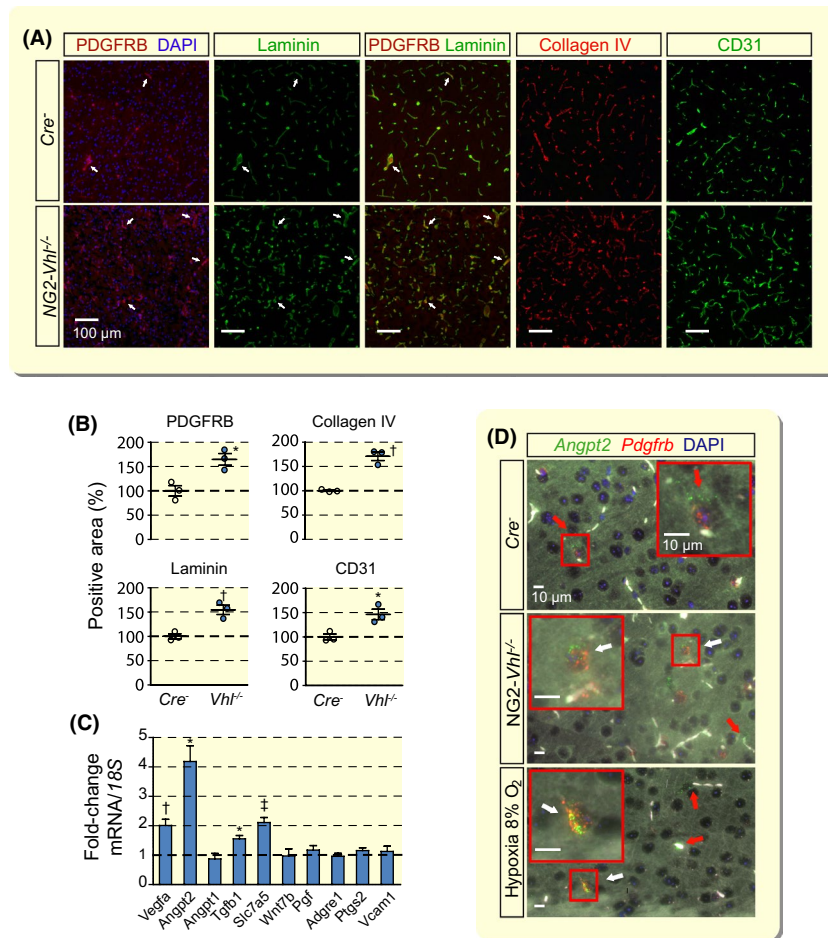


**FIGURE 1** *Vhl* inactivation in NG2 cells results in neurovascular remodelling and expansion. A, Representative immunofluorescence (IF) images of frozen brain sections from *Cre*<sup>-</sup> control and *NG2-Vhl*<sup>-/-</sup> mice (age 9–10 wk) stained for markers of pericytes (PDGFRB), basement membrane (laminin and collagen IV) and endothelial cells (CD31); cortex; scale bar, 100  $\mu$ m. Nuclei were stained with 4',6-diamidino-2-phenylindole (DAPI, blue fluorescence). There is complete overlap between PDGFRB and laminin IF staining. White arrows exemplify double-positive structures. B, Quantification of PDGFRB-, laminin-, collagen IV- and CD31-positive area expressed as percentage of *Cre*<sup>-</sup> control, (n = 3). C, Relative mRNA transcript levels in *NG2-Vhl*<sup>-/-</sup> cortex expressed as fold-change compared with *Cre*<sup>-</sup> control, (n = 3–5). D, Representative images of multiplex RNA FISH of cortical tissue from *Cre*<sup>-</sup> control, *NG2-Vhl*<sup>-/-</sup> and hypoxic wild-type mice (normobaric hypoxia, 8% O<sub>2</sub> for 24 h) detecting *angiopoietin 2* (green fluorescent signal) and *Pdgfrb*-expressing cells (red fluorescent signal). White arrows depict cells positive for both *Angpt2* and *Pdgfrb*; red arrows depict cells in the direct vicinity of micro-vessels that are positive for *Angpt2* and negative for *Pdgfrb*. White structures represent auto-fluorescent red blood cells. Nuclei were stained with DAPI (blue fluorescent signal); scale bar, 10  $\mu$ m. Data are represented as mean  $\pm$  SEM; two-tailed Student's *t* test; \**P* < .05, †*P* < .01 and ‡*P* < .001 compared with *Cre*<sup>-</sup> control. *Adgre1*, adhesion G-protein-coupled receptor E1; *Angpt1*, angiopoietin 1; *Angpt2*, angiopoietin 2; *Pgf*, placental growth factor; *Ptgs2*, prostaglandin-endoperoxide synthase 2; *Slc7a5*, solute carrier 7a5; *Tgfb1*, transforming growth factor beta 1; *Vcam1*, vascular cell adhesion molecule 1; *Vegfa*, vascular endothelial growth factor A; *Wnt7b*, wingless-type MMTV integration site family, member 7B

*Vhl* inactivation results in robust HIF activation because of complete abrogation of HIF $\alpha$  degradation.<sup>4</sup> We took advantage of transgenic mice that express Cre-recombinase under control of the *Ng2* promoter and generated *Ng2-cre Vhl*<sup>fllox/flox</sup> mice, which from hereon are referred to as *NG2-Vhl*<sup>-/-</sup> mutants. *Ng2-cre* targets brain pericytes and NG2 glia.<sup>14,25</sup>

*NG2-Vhl*<sup>-/-</sup> mutant mice had a normal life span and were characterized by elevated red blood cell (rbc) counts from increased EPO production.<sup>14</sup> As part of the initial morphological analysis, we performed immunofluorescence (IF) staining for PDGFRB in brains from adult *NG2-Vhl*<sup>-/-</sup> mutant and

*Cre*<sup>-</sup> littermate control mice (9–10 weeks old). PDGFRB is a commonly utilized molecular marker for pericytes and is specific for pericytes in the brain.<sup>29</sup> IF staining demonstrated a 65% increase in the area positive for PDGFRB staining (Figure 1A,B). To investigate whether increased PDGFRB staining resulted from an increase in pericyte numbers, we performed high-resolution fluorescence RNA in situ hybridization (RNA FISH) in conjunction with nuclear 4',6-diamidino-2-phenylindole (DAPI) staining. RNA FISH revealed a 90% increase in the number of *Pdgfrb*<sup>+</sup> cells in cortex compared to control (Figure S1A). Because pericytes modulate

endothelial cell behaviour and function,<sup>15,18,20</sup> we next investigated capillary density by IF staining for cluster differentiation antigen 31 (CD31). CD31 immunostaining revealed an increase in capillary area by ~50% in NG2-*Vhl*<sup>-/-</sup> mutants compared with control. Furthermore, capillary bed expansion was associated with a ~50% increase in the area positive for collagen type IV and laminin, both markers of basement membranes, in which endothelial cells and pericytes are typically embedded (Figure 1A,B).

To further corroborate our findings, we performed IF staining for a second pericyte marker, NG2. Because it has been reported that NG2 is also expressed by oligodendrocyte precursor cells,<sup>26</sup> we performed double IF staining for NG2 and CD31 to discriminate between NG2 pericytes and NG2 glia; capillary pericytes are in close proximity to endothelial cells and extend cellular processes along and around capillaries.<sup>15</sup> Combined NG2/CD31 staining demonstrated that NG2 expression was only associated with CD31-positive structures and was consistent with IF results for PDGFRB and CD31 double staining (Figure S1B). Taken together our combined IF and RNA FISH data indicate that the expansion of cerebral capillary beds in NG2-*Vhl*<sup>-/-</sup> mice was associated with an increase in the number of pericytes.

Cerebral vasculature expansion in NG2-*Vhl*<sup>-/-</sup> mice was furthermore associated with significantly increased transcript levels of angiogenic factors, such as *vascular endothelial growth factor A* (*Vegfa*), *angiopoietin 2* (*Angpt2*), *transforming growth factor beta 1* (*Tgfb1*) and *solute carrier 7a5* (*Slc7a5*), with increased phosphorylation of focal adhesion kinase (FAK) at tyrosine residue 576 (phospho-FAK576) and with enhanced activity of matrix metalloproteinase 9 (MMP-9) (Figure 1C and Figure S1C,D).

The strongest mRNA induction (~4-fold) was observed for *Angpt2*, which has been shown to be highly expressed in regions of vascular remodelling.<sup>30</sup> Although *Angpt2* is predominantly found in endothelial cells, expression in perivascular cells has been proposed.<sup>30,31</sup> To examine if *Angpt2* is expressed in pericytes we performed multiplex RNA FISH in NG2-*Vhl*<sup>-/-</sup> mutants with probes detecting *Angpt2* and *Pdgfrb* mRNA. RNA FISH detected a ~6-fold increase in the total number of *Angpt2*/*Pdgfrb* double-positive cells in the cerebral cortex compared to control, which was associated with an increase in the percentage of *Angpt2*-expressing pericytes (2.8 ± 1.1% for control and 14.8 ± 1.7% for NG2-*Vhl*<sup>-/-</sup> mice). In order to examine *Angpt2* in a more physiological model, we exposed mice to normobaric hypoxia (8% O<sub>2</sub> for 24 hours) and performed multiplex RNA FISH (Figure 1D). We found that *Angpt2* expression was restricted to vascular structures, where it is expressed in endothelium and pericytes, and observed a ~3-fold increase in the percentage of *Angpt2*-expressing pericytes in cerebral cortex, which is in line with findings from NG2-*Vhl*<sup>-/-</sup> mutants (data not shown). Taken together these results demonstrate that

pericytes in the murine cerebral cortex respond to hypoxia with the induction of *Angpt2*.

Similar to cortex, increased angiogenic gene expression, capillary density and pericyte numbers were also found in striatum and hypothalamus from NG2-*Vhl*<sup>-/-</sup> mice (Figures S1 and S2 and data not shown). We furthermore performed in situ zymography in conjunction with IF and found that the activity of MMP-9 co-localized with NG2 expression in the striatum (Figure S2C). This finding suggested that MMP-9 enzymatic activity was contained within the vascular compartment in pericytes. Increased MMP-9 activity is a key feature of vascular remodelling and angiogenesis,<sup>32</sup> and has been shown to be induced by hypoxia.<sup>13</sup>

To assess whether neurovascular expansion and remodelling in NG2-*Vhl*<sup>-/-</sup> mice resulted from inflammation, we assessed the expression of genes involved in the regulation of inflammation and endothelial cell activation. The expression of *prostaglandin-endoperoxide synthase 2* (*Ptgs2*, also known as *Cox-2*), *adhesion G-protein-coupled receptor E1* (*Adgre1* or *F4/80*) or *vascular cell adhesion molecule 1* (*Vcam-1*) was not increased in the brain from NG2-*Vhl*<sup>-/-</sup> mice, suggesting that the neurovascular phenotype of NG2-*Vhl*<sup>-/-</sup> mice is unlikely to result from neuroinflammation (Figure 1C).

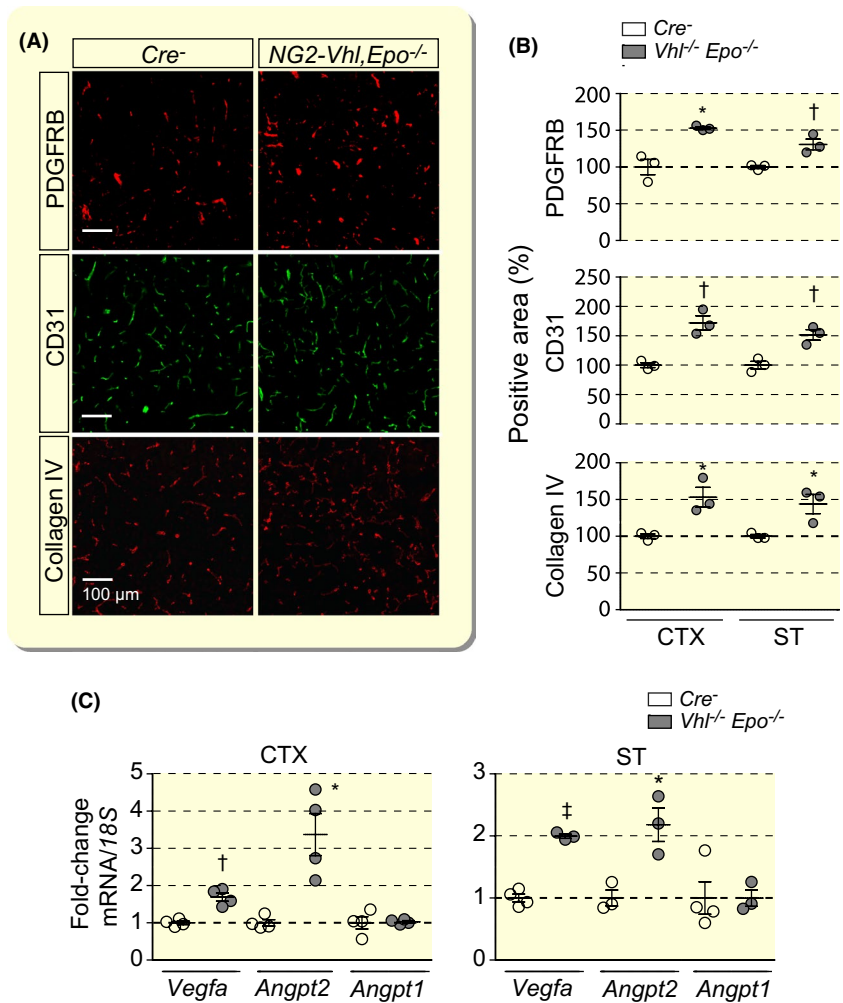
In summary, our findings demonstrate that *Vhl* inactivation in NG2 cells induced molecular changes consistent with vascular remodelling and resulted in the expansion of cerebral capillary beds, which was associated with an increase in pericyte numbers.

## 2.2 | Vascular expansion in NG2-*Vhl*<sup>-/-</sup> mice is not EPO-dependent

We have previously reported that NG2-*Vhl*<sup>-/-</sup> mice express increased levels of EPO in the brain,<sup>14</sup> which is known to have pro-angiogenic effects.<sup>33-35</sup> Therefore, we hypothesized that vascular expansion observed in NG2-*Vhl*<sup>-/-</sup> mice could have been partially induced by paracrine effects of EPO on endothelial cells. To test this hypothesis, we generated NG2-*Vhl*<sup>-/-</sup>*Epo*<sup>-/-</sup> double mutant mice, in which brain and serum EPO were no longer elevated.<sup>14</sup> We used IF staining to characterize the neurovasculature in NG2-*Vhl*<sup>-/-</sup>*Epo*<sup>-/-</sup> mutants by analysing the expression of molecular markers for pericytes (PDGFRB), endothelial cells (CD31) and basement membrane (collagen IV) (Figure 2A). NG2-*Vhl*<sup>-/-</sup>*Epo*<sup>-/-</sup> mice were characterized by increased capillary density in both cerebral cortex and striatum as assessed by CD31 staining and were not significantly different from NG2-*Vhl*<sup>-/-</sup> mice (172 ± 12.11% vs 146 ± 16.65%) (Figure 2B). Moreover, the expression of angiogenic genes was increased in cortex and striatum from NG2-*Vhl*<sup>-/-</sup>*Epo*<sup>-/-</sup> mice and was comparable in magnitude to NG2-*Vhl*<sup>-/-</sup> mutants (Figure 2C). Taken together,



**FIGURE 2** Cerebral vascular expansion in NG2-*Vhl*<sup>-/-</sup> mutant mice is not EPO-dependent. A, Representative immunofluorescence images of frozen brain sections from *Cre*<sup>-</sup> control and NG2-*Vhl*<sup>-/-</sup>*Epo*<sup>-/-</sup> (*Vhl*<sup>-/-</sup>*Epo*<sup>-/-</sup>) mice stained for markers of pericytes (PDGFRB), endothelial cells (CD31) and basement membrane (collagen IV); shown is cortex; scale bar, 100  $\mu$ m. B, Quantification of cortical and striatal PDGFRB-, CD31- and collagen IV-positive areas expressed as percentage of *Cre*<sup>-</sup> control, (n = 3). C, Relative mRNA levels in cerebral cortex (CTX) and striatum (ST) from NG2-*Vhl*<sup>-/-</sup>*Epo*<sup>-/-</sup> mice expressed as fold-change compared with *Cre*<sup>-</sup> control, (n = 4). Data are represented as mean  $\pm$  SEM; two-tailed Student's *t* test; \**P* < .05, †*P* < .01 and ‡*P* < .001. *Angpt1*, angiotensinogen 1; *Angpt2*, angiotensinogen 2; *Vegfa*, vascular endothelial growth factor A



our data suggest that EPO does not play a significant role in neurovascular expansion and remodelling induced by *Vhl* gene inactivation in NG2 cells.

### 2.3 | Combined inactivation of *Phd2* and *Phd3* but not inactivation of *Phd2* alone is associated with neurovascular expansion

Although the VHL protein is an integral part of the HIF oxygen sensing machinery, it is not an oxygen sensor *sensu stricto*. Therefore, we next investigated the role of individual HIF-PHD oxygen sensors in the regulation of neurovascular homeostasis. For this, we generated mice with individual or combined conditional inactivation of *Phd1*, *Phd2* and *Phd3* using *Ng2-cre* transgenic mice. Because PHD2 inactivation alone is sufficient for HIF $\alpha$  stabilization in many cell types, where it functions as the main HIF-prolyl 4-hydroxylase, we first evaluated the cerebral vasculature of NG2-*Phd2*<sup>-/-</sup> animals.<sup>6,36</sup> Surprisingly, genetic inactivation of *Phd2* did not result in pericyte, endothelial cell or basement membrane expansion as assessed by IF for PDGFRB, CD31 and collagen IV (Figure 3A,B).

Consistent with the lack of a vascular phenotype, transcript levels of *Vegfa*, *Angpt2*, *Angpt1*, *Tgfb1*, *fibroblast growth factor 2* (*Fgf2*) or *C-X-C motif chemokine 12* (*Cxcl12*) were not increased in cerebral cortex from NG2-*Phd2*<sup>-/-</sup> mutants (Figure 3C).

Because *Phd3* transcript levels were increased in whole tissue homogenates from different NG2-*Phd2*<sup>-/-</sup> brain regions, which contained a mixture of *Phd2*-deficient and non-deficient cell types (Figure 3D), we hypothesized that increased PHD3 catalytic activity may have compensated for the loss of PHD2 function preventing the activation of HIF signalling. To test this hypothesis, we generated and characterized NG2-*Phd2*<sup>-/-</sup>*Phd3*<sup>-/-</sup> double-mutant mice. IF analysis of frozen sections for pericyte, endothelial cell and basement membrane markers PDGFRB, CD31 and collagen IV revealed a significant expansion in capillary density, pericyte numbers and basement membrane area in cortex compared with control (Figure 3A,B).

Taken together, our data demonstrate that PHD2 function loss in NG2 cells alone is not sufficient for HIF activation and suggest that increased *Phd3* expression is capable of compensating for the loss of PHD2 catalytic activity in NG2 cells.

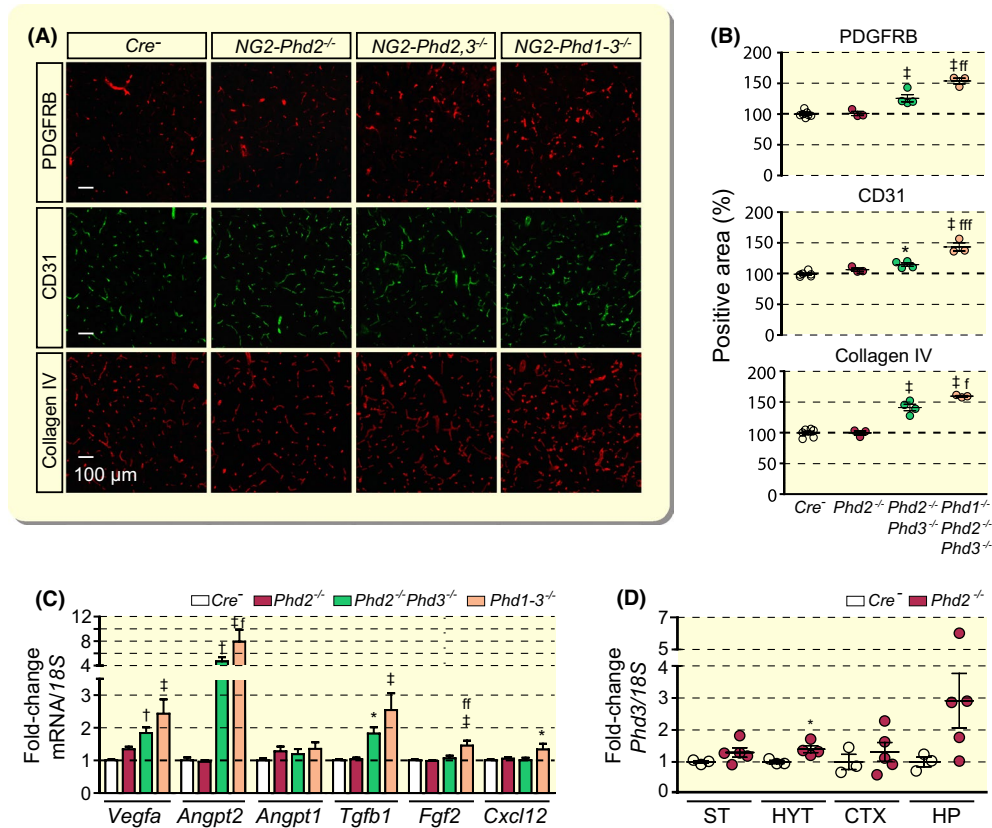


**FIGURE 3** Combined inactivation of *Phd2* and *Phd3* but not inactivation of *Phd2* alone promotes cerebral vascular expansion. A, Representative immunofluorescent images of frozen brain sections from *Cre*<sup>-</sup> control, *NG2-Phd2*<sup>-/-</sup>, *NG2-Phd2*<sup>-/-</sup>*Phd3*<sup>-/-</sup> (*NG2-Phd2,3*<sup>-/-</sup>) and *NG2-Phd1*<sup>-/-</sup>*Phd2*<sup>-/-</sup>*Phd3*<sup>-/-</sup> (*NG2-Phd1-3*<sup>-/-</sup>) mice stained for PDGFRB, CD31 and collagen IV; scale bar, 100  $\mu$ m. B, Quantification of cortical PDGFRB-, CD31- and collagen IV-positive areas expressed as percentage of *Cre*<sup>-</sup> control (n = 3-6). C, Relative cortical mRNA transcript levels in homogenates from cortex of *Cre*<sup>-</sup> control, *NG2-Phd2*<sup>-/-</sup>, *NG2-Phd2*<sup>-/-</sup>*Phd3*<sup>-/-</sup> and *NG2-Phd1*<sup>-/-</sup>*Phd2*<sup>-/-</sup>*Phd3*<sup>-/-</sup> mice expressed as fold-change compared to *Cre*<sup>-</sup> control (n = 4-11). D, *Phd3* transcript levels in striatum (ST), hypothalamus (HYT); cortex (CTX) and hippocampus (HP) from *Cre*<sup>-</sup> control and *NG2-Phd2*<sup>-/-</sup> mice. Data are represented as mean  $\pm$  SEM; one-way ANOVA followed by Tukey's post hoc analysis; \**P* < .05, <sup>†</sup>*P* < .01 and <sup>‡</sup>*P* < .001 compared with *Cre*<sup>-</sup> control; <sup>††</sup>*P* < 0.05, <sup>†††</sup>*P* < 0.01, and <sup>††††</sup>*P* < 0.001 compared with *NG2-Phd2*<sup>-/-</sup>*Phd3*<sup>-/-</sup> mice. *Angpt1*, angiotensinogen 1; *Angpt2*, angiotensinogen 2; *Cxcl12*, C-X-C motif chemokine 12; *Fgf2*, fibroblast growth factor 2; *Tgfb1*, transforming growth factor beta 1; *Vegfa*, vascular endothelial growth factor A

## 2.4 | PHD1 modulates neurovascular expansion in *NG2-Phd2*<sup>-/-</sup>*Phd3*<sup>-/-</sup> double mutants

To gain insights into the role of the third HIF-prolyl 4-hydroxylase, PHD1, in the regulation of neurovascular homeostasis, we co-inactivated *Phd1* in *NG2-Phd2*<sup>-/-</sup>*Phd3*<sup>-/-</sup> mice. *NG2-Phd1*<sup>-/-</sup>*Phd2*<sup>-/-</sup>*Phd3*<sup>-/-</sup> triple mutant animals were characterized by a significant increase in capillary density compared with *NG2-Phd2*<sup>-/-</sup>*Phd3*<sup>-/-</sup> mice (Figure 3A,B). These phenotypic changes were associated with a further increase in angiogenic gene expression (Figure 3C). Additional increases were observed for *Vegfa*, *Angpt2* and *Tgfb1* compared with *NG2-Phd2*<sup>-/-</sup>*Phd3*<sup>-/-</sup> mutants, whereas *Fgf2* and *Cxcl12* transcript levels were only elevated in *NG2-Phd1*<sup>-/-</sup>*Phd2*<sup>-/-</sup>*Phd3*<sup>-/-</sup> triple mutant brains and not in *NG2-Phd2*<sup>-/-</sup>*Phd3*<sup>-/-</sup> double mutants (Figure 3C). Thus, our findings establish that, although combined *Phd2/Phd3* inactivation in NG2 cells is sufficient for

the induction of angiogenic gene expression and neurovascular expansion, neurovascular expansion is submaximal in *NG2-Phd2*<sup>-/-</sup>*Phd3*<sup>-/-</sup> brains and can be further stimulated by the additional co-inactivation of *Phd1*.

## 2.5 | Combined inactivation of *Phd2* and *Phd3* in NG2 cells is associated with pericyte proliferation

We next investigated to what degree neurovascular expansion in *NG2-Phd2*<sup>-/-</sup>*Phd3*<sup>-/-</sup> and *NG2-Phd1*<sup>-/-</sup>*Phd2*<sup>-/-</sup>*Phd3*<sup>-/-</sup> mice was associated with vascular cell proliferation. We performed IF staining for proliferation marker antigen Ki 67 (Ki67) and quantified the number of cortical Ki67<sup>+</sup> nuclei per tissue area. As shown in Figure 4, co-inactivation of *Phd2* and *Phd3* was associated with a significant increase in the total number of

Ki67<sup>+</sup> nuclei in cerebral cortex compared with control ( $6.14 \pm 0.095$  vs  $5.13 \pm 0.188$  Ki67<sup>+</sup> cells mm<sup>-2</sup> in control). Co-inactivation of *Phd1* resulted in an additional increase in Ki67<sup>+</sup> cells compared with NG2-*Phd2*<sup>-/-</sup>-*Phd3*<sup>-/-</sup> mice ( $7.342 \pm 0.479$  Ki67<sup>+</sup> cells mm<sup>-2</sup>). Because the total number of Ki67<sup>+</sup> cells was increased in NG2-*Phd2*<sup>-/-</sup>-*Phd3*<sup>-/-</sup> and NG2-*Phd1*<sup>-/-</sup>-*Phd2*<sup>-/-</sup>-*Phd3*<sup>-/-</sup> mice, we next examined whether Ki67 expression was co-localized with pericyte marker PDGFRB and performed double IF staining for both PDGFRB and Ki67 (Figure 4A). NG2-*Phd2*<sup>-/-</sup>-*Phd3*<sup>-/-</sup> and NG2-*Phd1*<sup>-/-</sup>-*Phd2*<sup>-/-</sup>-*Phd3*<sup>-/-</sup> mice were characterized by a significant increase in the number of PDGFRB<sup>+</sup>Ki67<sup>+</sup> cells compared with *Cre*<sup>-</sup> control ( $2.079 \pm 0.195$  and  $2.860 \pm 0.209$  cells mm<sup>-2</sup>, respectively, vs  $0.639 \pm 0.07$  cells mm<sup>-2</sup> in control) as well as increase in the fraction of PDGFRB<sup>+</sup>/Ki67<sup>+</sup> cells within the Ki67<sup>+</sup> cell population (33.6% and 38.9%, respectively, vs 12.9% in *Cre*<sup>-</sup> control) (Figure 4B). Furthermore, the PDGFRB Ki67-double-positive cell number correlated well with the size of the PDGFRB-positive area (Pearson's *r* value of 0.8895 with *P* = .0002) suggesting that pericyte expansion in *Phd* double and triple mutants was associated with pericyte proliferation (Figure 4B). Taken together, our data indicate that the combined *Phd* inactivation not only results in an expansion of the neurovascular capillary bed but also induces pericyte proliferation.

## 2.6 | Neurovascular expansion in NG2-*Phd1*<sup>-/-</sup>-*Phd2*<sup>-/-</sup>-*Phd3*<sup>-/-</sup> mutant mice requires HIF2 signalling

HIF-PHD dioxygenases target oxygen-sensitive HIF $\alpha$  subunits for proteasomal degradation via hydroxylation of specific proline residues. Because we have previously shown that EPO induction in NG2 pericytes was completely HIF2-dependent,<sup>14</sup> we examined the role of HIF2 in neurovascular expansion by crossing the *Hif2a* conditional allele into the NG2-*Phd1*<sup>-/-</sup>-*Phd2*<sup>-/-</sup>-*Phd3*<sup>-/-</sup> background. Homozygous deletion of *Hif2a* in NG2-*Phd1*<sup>-/-</sup>-*Phd2*<sup>-/-</sup>-*Phd3*<sup>-/-</sup> mice reduced capillary density and pericyte proliferation to baseline levels (Figure 5A-C) and normalized angiogenic gene expression completely (Figure 5D). Consistent with HIF2 dependence is the increased abundance of *Hif2a* transcripts in brain pericytes (~13-fold difference compared with *Hif1a*) as determined by single-cell RNA sequencing (Figure S3A), and the significantly larger number of HIF2 $\alpha$ -expressing perivascular cells detected by immunohistochemistry (IHC) in NG2-*Phd1*<sup>-/-</sup>-*Phd2*<sup>-/-</sup>-*Phd3*<sup>-/-</sup> brains compared with HIF1 $\alpha$ ,  $46.84 \pm 2.20$  cells mm<sup>-2</sup> for HIF2 $\alpha$  vs  $6.59 \pm 1.84$  cells mm<sup>-2</sup> for HIF1 $\alpha$  (Figure S3B). Taken together, our data demonstrate that HIF2 is required for the induction of angiogenic gene expression and expansion of neurovascular

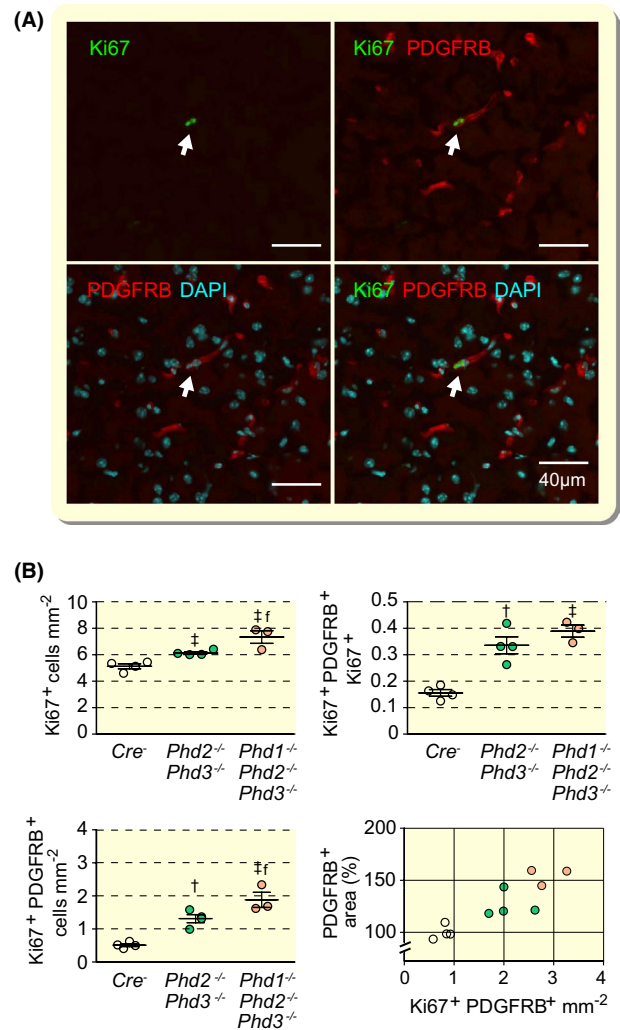


**FIGURE 4** Combined inactivation of *Phd2* and *Phd3* in NG2 cells promotes pericyte proliferation. A, Representative high-power immunofluorescence images of proliferating pericytes in cerebral cortex depicted by white arrows. PDGFRB-positive cells are identified by red fluorescence and proliferating cells by Ki67 staining (green fluorescent signal). Nuclei were stained with 4',6-diamidino-2-phenylindole (DAPI, blue fluorescence); scale bar, 40 μm. B, Quantification of cells in cerebral cortex from *Cre*<sup>-</sup> control, NG2-*Phd2*<sup>-/-</sup>-*Phd3*<sup>-/-</sup> and NG2-*Phd1*<sup>-/-</sup>-*Phd2*<sup>-/-</sup>-*Phd3*<sup>-/-</sup> mice; (age 9–10 wk, n = 3–4). Left upper panel, Ki67<sup>+</sup> cells; left lower panel, proliferating pericytes (Ki67<sup>+</sup>PDGFRB<sup>+</sup>); right upper panel, ratio of Ki67<sup>+</sup>PDGFRB<sup>+</sup> cells over total number of Ki67<sup>+</sup> cells; right lower panel, correlation between pericyte covered area (PDGFRB<sup>+</sup> cells) and proliferating pericytes; *Cre*<sup>-</sup> control (empty circles); NG2-*Phd2*<sup>-/-</sup>-*Phd3*<sup>-/-</sup> (green circles); NG2-*Phd1*<sup>-/-</sup>-*Phd2*<sup>-/-</sup>-*Phd3*<sup>-/-</sup> mice (coral-colored circles); Pearson's *r* = 0.8895, *P* = .0002 (two-tailed). Data are represented as mean ± SEM; one-way ANOVA followed by Tukey's post hoc analysis, <sup>†</sup>*P* < .01 and <sup>‡</sup>*P* < .001 compared with *Cre*<sup>-</sup> controls. <sup>§</sup>*P* < 0.05 compared with NG2-*Phd2*<sup>-/-</sup>-*Phd3*<sup>-/-</sup> mice

capillary beds in mice with combined inactivation of *Phd1*, *Phd2* and *Phd3* in NG2 cells. Furthermore, our studies suggest that HIF2 $\alpha$  is the predominant HIF $\alpha$  subunit in NG2-expressing cerebral perivascular cells.



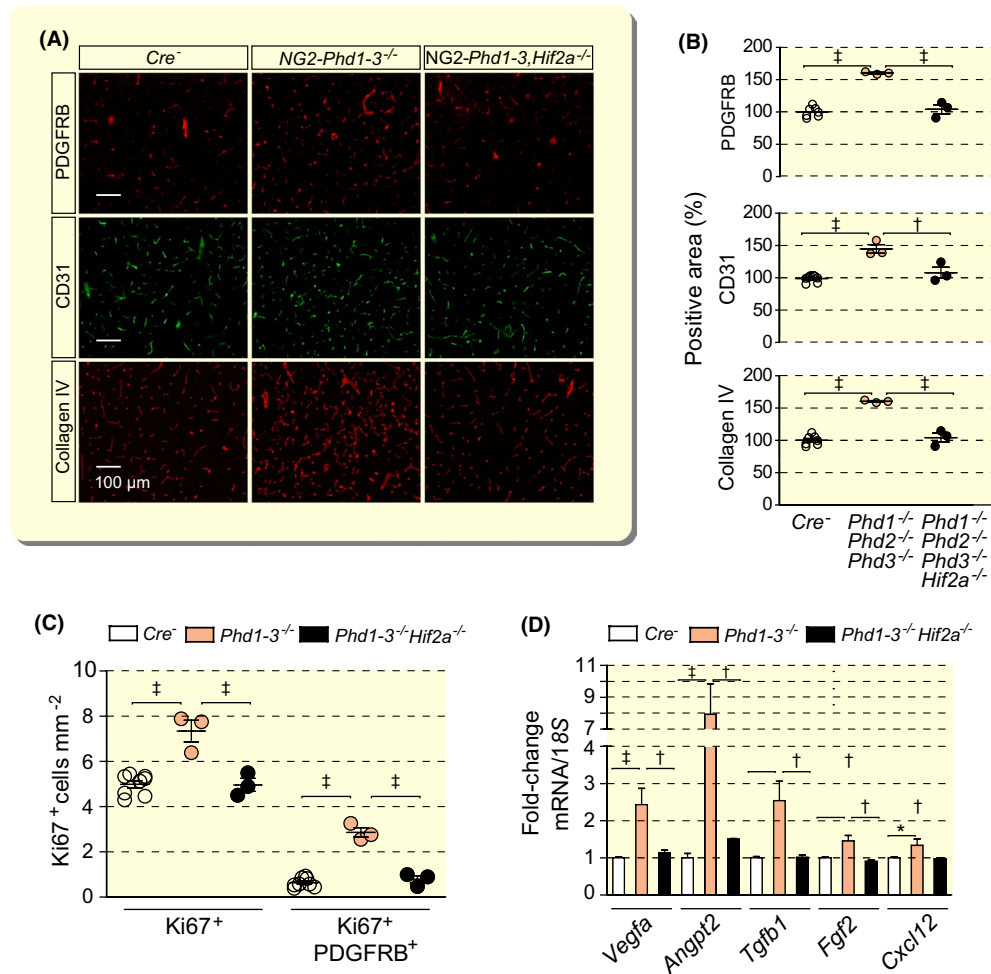


**FIGURE 5** Vascular expansion and pericyte proliferation in mice with combined *Phd1*, *Phd2*, *Phd3* deletion is HIF2-dependent. A, Representative immunofluorescence images of frozen brain sections from *Cre*<sup>-</sup> control, *NG2-Phd1*<sup>-/-</sup> *Phd2*<sup>-/-</sup> *Phd3*<sup>-/-</sup> (*Phd1-3*<sup>-/-</sup>) and *NG2-Phd1*<sup>-/-</sup> *Phd2*<sup>-/-</sup> *Phd3*<sup>-/-</sup> *Hif2a*<sup>-/-</sup> (*Phd1-3*<sup>-/-</sup> *Hif2a*<sup>-/-</sup>) mice stained for markers of pericytes (PDGFRB), endothelial cells (CD31) and basement membrane (collagen IV); scale bar, 100  $\mu$ m. B, Quantification of cortical PDGFRB-, CD31- and collagen IV-positive areas expressed as percentage of *Cre*<sup>-</sup> control, (n = 3-8). C, Quantification of proliferating cells (Ki67<sup>+</sup>) and proliferating pericytes (Ki67<sup>+</sup> PDGFRB<sup>+</sup>) in cerebral cortex from *Cre*<sup>-</sup> control, *NG2-Phd1*<sup>-/-</sup> *Phd2*<sup>-/-</sup> *Phd3*<sup>-/-</sup> and *NG2-Phd1*<sup>-/-</sup> *Phd2*<sup>-/-</sup> *Phd3*<sup>-/-</sup> *Hif2a*<sup>-/-</sup> mice, (n = 3-8). D, Relative mRNA levels in cortex homogenates from *Cre*<sup>-</sup> control, *NG2-Phd1*<sup>-/-</sup> *Phd2*<sup>-/-</sup> *Phd3*<sup>-/-</sup> and *NG2-Phd1*<sup>-/-</sup> *Phd2*<sup>-/-</sup> *Phd3*<sup>-/-</sup> *Hif2a*<sup>-/-</sup> mice, (n = 3-8). Data are represented as mean  $\pm$  SEM; one-way ANOVA followed by Tukey's post hoc analysis, \**P* < .05, <sup>†</sup>*P* < .01 and <sup>‡</sup>*P* < .001 compared with *Cre*<sup>-</sup> controls, <sup>ff</sup>*P* < 0.01 and <sup>fff</sup>*P* < 0.001 compared with *NG2-Phd1*<sup>-/-</sup> *Phd2*<sup>-/-</sup> *Phd3*<sup>-/-</sup> mice. *Angpt2*, angiotensinogen; *Cxcl12*, C-X-C motif chemokine 12; *Fgf2*, fibroblast growth factor 2; *Tgfb1*, transforming growth factor beta 1; *Vegfa*, vascular endothelial growth factor A

### 3 | DISCUSSION

Here we have used cell-type-specific gene targeting in mice to investigate the role of the HIF/PHD/VHL axis in neurovascular homeostasis. We demonstrate that HIF2 activation in NG2 cells induces a pronounced expansion and remodelling of the cerebral vasculature via the induction of pro-angiogenic genes. Furthermore, our studies examine the role of individual HIF-prolyl 4-hydroxylases in neurovascular homeostasis and characterize their contributions to the regulation of HIF2-dependent gene transcription. In addition, our data do not support a significant role for EPO in HIF2-induced neurovascular expansion and remodelling.

We used *Ng2-cre* transgenic mice to target the HIF/PHD/VHL axis in NG2 cells. Although NG2 is a widely used marker of pericytes,<sup>20</sup> NG2 glia, which give rise to a subpopulation of oligodendrocytes, are also contained within the NG2 cell population.<sup>26</sup> Notwithstanding this observation, we found strong colocalization between NG2 and PDGFRB, and NG2 and CD31 by IF staining, suggesting that NG2 in the adult mouse brain is predominantly expressed in cerebral pericytes. *Ng2-cre*-mediated recombination, however, is predicted to occur in all cells with a history of NG2 expression and their progeny, and has been observed in pericytes and some oligodendrocytes.<sup>14,25</sup>

Pericytes are essential for vascular homeostasis as their ablation results in loss of cerebral vascularity and disruption



of the blood brain barrier.<sup>37</sup> Pericytes express matrix metalloproteinases that enhance matrix degradation and facilitate endothelial cell migration and the release of angiogenic factors stored in the extracellular matrix.<sup>38</sup> Furthermore, pericytes secrete TGF $\beta$ 1, which activates the endothelial activin-like receptor kinase 1 (ALK1)/mothers against decapentaplegic homolog (SMAD) 1,5,8 pathway promoting endothelial cell proliferation and migration.<sup>39</sup> Consistent with these observations, we detected increased perivascular MMP-9 activity in cortex and striatum from NG2-*Vhl*<sup>-/-</sup> mice by zymography as well as increased *Tgfb1* transcript levels in NG2-*Vhl*<sup>-/-</sup> and *Phd* double and triple mutants. We also found that HIF2 activation in NG2 pericytes induced *Angpt2*, which encodes the vascular growth factor angiopoietin 2. Angiopoietin 2 is a pro-angiogenic ligand for the TEK receptor tyrosine kinase (TIE2) and plays a context-dependent competitive antagonistic or agonistic role in TIE2 receptor autophosphorylation and signalling.<sup>30,40,41</sup> Because the TIE2 receptor, which is expressed in both, endothelial cells and NG2 pericytes, has been shown to control angiogenesis and vessel maturation,<sup>42,43</sup> our data suggest that pericyte-derived angiopoietin 2 most likely has contributed to the pro-angiogenic phenotype in our models through autocrine mechanisms and/or paracrine effects on endothelial cells. Our RNA FISH studies provide clear evidence that brain pericytes are sources of angiopoietin 2 under conditions of hypoxia and genetic HIF activation. This had not been clearly established in previous studies.<sup>30</sup>

Genetic studies in mice have suggested that NG2 glia contribute to neurovascular homeostasis. Diphteria toxin-mediated deletion of NG2 glia using *Ng2-cre* transgenic mice resulted in a reduction in cerebral vasculature and supported a role for NG2 glia in cerebral angiogenesis.<sup>19</sup> In addition, HIF $\alpha$  stabilization in *Vhl*-deficient *Sox10*- and *Olig1*-expressing cells led to the activation of Wnt7a/7b signalling and promoted cerebral angiogenesis.<sup>44</sup> *Vhl* deletion in this model was associated with tremor, ataxia and juvenile lethality by postnatal day 21. In contrast, our studies in NG2 cells did not result in Wnt7 activation and did not produce any visible neurological dysfunction in adult mice nor result in premature death. This discrepancy in phenotypes may be a reflection of differences in timing of HIF activation or in the cell populations that were targeted by *Sox10-cre*, *Olig1-cre* and *Ng2-cre* transgenes. Although it is difficult to assess the relative contribution of NG2 glia to the vascular phenotype in our model, we did neither observe *Angpt2* expression nor increased MMP-9 activity in non-vascular cells or structures, suggesting that NG2 pericytes have played a predominant role in the development of the neurovascular phenotype in our models.

Cells synthesize HIF $\alpha$  continuously. Under normoxia the rate of HIF $\alpha$  synthesis and proteasomal degradation, which is initiated by prolyl 4-hydroxylation, are in balance, resulting in non-detectable or very low cellular HIF $\alpha$  levels. Prolyl

4-hydroxylation of HIF- $\alpha$  is executed by three 2-oxoglutarate-dependent dioxygenases, PHD1, PHD2 and PHD3.<sup>4</sup> Among these, PHD2 is the main dioxygenase that regulates HIF under normoxia, as inactivation of PHD2 alone results in significant HIF activation in many cell types.<sup>6-8</sup> This notion is furthermore supported by genetic studies in mice, where germline inactivation of *Phd2* resulted in embryonic lethality,<sup>36,45</sup> whereas mice with *Phd1* or *Phd3* germline deficiency were viable.<sup>45</sup> However, in some cell populations robust induction of HIF target genes can only be achieved by simultaneous inhibition of all three PHDs.<sup>46</sup>

Here, we show that the neurovascular phenotype in *Phd* knockout mice requires either the combined inactivation of *Phd2* together with *Phd3* or the combined inactivation of *Phd2* together with both *Phd3* and *Phd1* (overview in Figure 6). In contrast, the combined inactivation of *Phd1* and *Phd2* did not result in significant HIF activation (data not shown). The most likely explanation for this finding is that, under conditions of reduced or absent PHD2 function, PHD3 generates sufficient hydroxylation activity to maintain the balance between HIF $\alpha$  synthesis and degradation, thus preventing cellular HIF $\alpha$  accumulation. PHD3 itself is hypoxia-regulated, and HIF is predicted to increase PHD3 levels and thus hydroxylation activity, providing the basis for an autoregulatory feed-back loop that readjusts the set-point for HIF activation and fine tunes hypoxia responses.<sup>8,47,48</sup> In support of this notion are our findings in NG2-*Phd2* knock-out mice, where significant increases in *Phd3* transcript levels were found in several anatomic subregions of the brain. Mice, which are globally deficient for either *Phd1* or *Phd3* do not develop a significant vascular phenotype.<sup>45,49</sup>

Co-deletion of *Phd1* enhanced the neurovascular phenotype of NG2-*Phd2*<sup>-/-</sup>*Phd3*<sup>-/-</sup> mice, further increased transcript levels of *Vegfa*, *Angpt2* and *Tgfb1*, and induced the expression of *Fgf2* and *Cxcl12*, which were not elevated in NG2-*Phd2*<sup>-/-</sup>*Phd3*<sup>-/-</sup> mutants compared with control. This is in contrast to the regulation of EPO in *Ng2-cre* mutants, where the additional deletion of *Phd1* in NG2-*Phd2*<sup>-/-</sup>*Phd3*<sup>-/-</sup> mice did not result in any further increase in *Epo* transcript levels.<sup>14</sup> Although we cannot completely rule out the possibility that PHD1 acts through HIF-independent mechanisms,<sup>50</sup> concomitant *Hif2a* inactivation, however, suggested that the neurovascular phenotype in NG2-*Phd1*<sup>-/-</sup>*Phd2*<sup>-/-</sup>*Phd3*<sup>-/-</sup> mice was completely HIF2-dependent. In support of this notion are recent studies, which indicate that HIF-PHDs are unlikely to hydroxylate targets other than HIF $\alpha$ .<sup>51</sup>

Our data establish that the neurovascular phenotype in NG2-*Phd1*<sup>-/-</sup>*Phd2*<sup>-/-</sup>*Phd3*<sup>-/-</sup> mice is completely HIF2-dependent. This is in line with IHC analysis of NG2-*Phd1*<sup>-/-</sup>*Phd2*<sup>-/-</sup>*Phd3*<sup>-/-</sup> brains, which demonstrated that the vast majority of perivascular cells expressed HIF2 $\alpha$  and not HIF1 $\alpha$ , and single-cell RNA sequencing analysis of mouse brains, which indicated that *Hif1a* transcript levels in

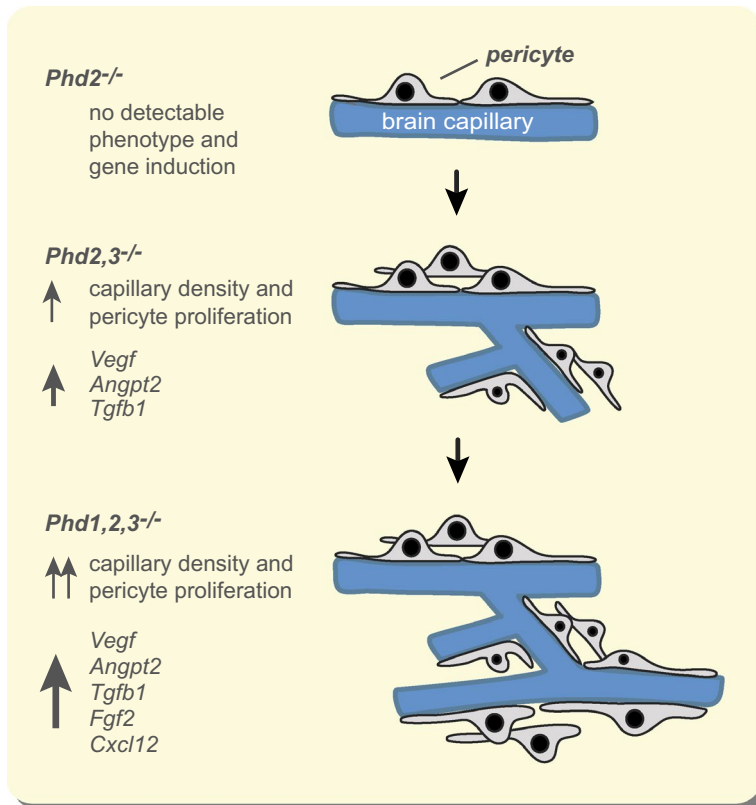


**FIGURE 6** Differential role of individual HIF-PHDs in the regulation of neurovascular homeostasis. Overview of findings in mice with *Phd* gene inactivation in NG2 cells. *Angpt2*, angiotensinogen 2; *Cxcl12*, C-X-C motif chemokine 12; *Fgf2*, fibroblast growth factor 2; *Tgfb1*, transforming growth factor beta 1; *Vegfa*, vascular endothelial growth factor A

brain pericytes are very low compared to *Hif2a*.<sup>52-54</sup> HIF2-dependence of oxygen-regulated gene expression in brain pericytes is not surprising as cells of the same histogenetic origin such as perivascular EPO-producing cells in the kidney also rely on HIF2 for the induction of transcriptional hypoxia responses.<sup>55,56</sup> However, a subset of perivascular cells in NG2-*Phd1*<sup>-/-</sup>*Phd2*<sup>-/-</sup>*Phd3*<sup>-/-</sup> brains expressed HIF1 $\alpha$ . Although HIF1 and HIF2 co-regulate a large number of genes, certain genes are predominantly HIF2-regulated, eg *EPO* and *OCT4*, whereas others are predominantly HIF1-dependent, such as genes encoding glycolytic enzymes.<sup>57</sup> It is therefore plausible that HIF1 $\alpha$ -expressing perivascular cells in the brain are functionally different from those that express HIF2 $\alpha$ .

Previous in vivo studies have shown that *Epo* is more sensitive to hypoxia compared to other oxygen-regulated genes such as *Vegfa*, as a lesser degree of hypoxia was required for the induction of *Epo*.<sup>58</sup> Differential sensitivity of gene transcription to HIF activation has also been demonstrated in cultured cells treated with small molecule HIF-PHD inhibitors (HIF-PHIs),<sup>59</sup> and in clinical studies in humans, where low doses of systemically administered HIF-PHIs were sufficient for the stimulation of endogenous EPO production but did not increase plasma VEGF levels.<sup>60</sup> Therefore, it is plausible that the induction of *Fgf2* and *Cxcl12* may require cellular HIF2 $\alpha$  levels that can only be generated by the combined inactivation of all three HIF-PHDs.

Because NG2-*Vhl*<sup>-/-</sup> mice express very high levels of EPO in the brain (~600 pg/mg tissue protein), which is mostly pericyte-derived,<sup>14</sup> we hypothesized that increased EPO production in pericytes could have significantly contributed to the vascular phenotype observed in NG2-*Vhl*<sup>-/-</sup> mice. EPO is known to be a pleiotropic cytokine that aside from stimulating rbc formation in the bone marrow, enhances angiogenesis and endothelial cell proliferation through EPO receptor activation in several tissues.<sup>33-35</sup> Furthermore, EPO may affect vascular homeostasis indirectly through an increase in blood viscosity, which is normally associated with elevated rbc counts.<sup>61</sup> However, the physiological relevance of these effects has been debated.<sup>62-65</sup> To investigate the potential role of pericyte-derived EPO in cerebral angiogenesis in NG2-*Vhl*<sup>-/-</sup> mice, we generated NG2-*Vhl*<sup>-/-</sup>*Epo*<sup>-/-</sup> mice. Surprisingly, simultaneous inactivation of *Epo* did neither impact neurovascular expansion nor affect angiogenic gene expression, although the expression of *Vegfa* and *Angpt2* had been reported to be modulated by EPO.<sup>66,67</sup> Our results are in line with previous studies, which suggested that EPO receptors in endothelial cells may not be detectable or functional.<sup>64</sup> Although our studies demonstrate that local EPO production was not required for HIF-induced neurovascular expansion in NG2-*Vhl*<sup>-/-</sup> mice, we cannot completely exclude minor effects on cerebral vasculogenesis or angiogenesis.

In summary, our data provide novel insights into the role of HIF oxygen sensing in neurovascular hypoxia responses.

Our data have implications not only for understanding normal physiology but are of relevance to neurological diseases, which are frequently associated with vascular atrophy and pericyte loss.<sup>68</sup> Our results are likely to stimulate further research into the role of oxygen metabolism in neurovascular function in health and disease.

## 4 | MATERIALS AND METHODS

### 4.1 | Generation and genotyping of mice and animal procedures

The generation and genotyping of mice expressing *Ng2-cre* and floxed alleles for *Vhl*, *Hif1a*, *Hif2a* (*Epas1*), *Epo*, *Phd1* (*Egln2*), *Phd2* (*Egln1*) and *Phd3* (*Egln3*) is described elsewhere.<sup>14,25</sup> Briefly, mice carrying floxed alleles were bred with *Ng2-cre* female mice. *Ng2-cre Vhl<sup>flox/flox</sup>*; *Ng2-cre Vhl<sup>flox/flox</sup> Epo<sup>flox/flox</sup>*; *Ng2-cre Phd2<sup>flox/flox</sup>*; *Ng2-cre Phd1<sup>flox/flox</sup> Phd2<sup>flox/flox</sup> Phd3<sup>flox/flox</sup>* and *Ng2-cre Phd1<sup>flox/flox</sup> Phd2<sup>flox/flox</sup> Phd3<sup>flox/flox</sup> Hif2a<sup>flox/flox</sup>* are referred to as *NG2-Vhl<sup>-/-</sup>*, *NG2-Vhl<sup>-/-</sup>Epo<sup>-/-</sup>*, *NG2-Phd1<sup>-/-</sup>Phd2<sup>-/-</sup>*, *NG2-Phd1<sup>-/-</sup>Phd2<sup>-/-</sup>Phd3<sup>-/-</sup>* and *NG2-Phd1<sup>-/-</sup>Phd2<sup>-/-</sup>Phd3<sup>-/-</sup>Hif2a<sup>-/-</sup>* mice respectively. Animals were exposed to 8% hypoxia as previously described.<sup>14</sup> Male and female mice aged 9–10 weeks were used for the analysis. All procedures involving mice were performed in accordance with NIH guidelines for the use and care of live animals and were approved by Vanderbilt University's Institutional Animal Care and Use Committee (IACUC).

### 4.2 | DNA and RNA analysis

DNA analysis for genotyping was performed as described previously.<sup>14</sup> RNA was isolated from different anatomic regions of the brain using the RNeasy kit according to the manufacturer's protocol (Qiagen, Valencia, CA, USA). Relative mRNA expression levels were assessed with qPCR and analysed with the relative standard curve method according to the manufacturer's instructions (Applied Biosystems, Foster City, CA, USA). *18S* rRNA was used for normalization. A detailed list of primer sequences used for qPCR can be found in Supplemental Materials and Methods (Table S1).

### 4.3 | Single cell RNA sequencing data analysis

scRNA seq analysis of mouse brains has been described previously.<sup>52,53</sup> Data were accessed at: <http://mousebrain.org/genesearch.html>. Search terms included *Hif1a*, *Epas1*, *Egln1/Phd2*, *Egln2/Phd1* and *Egln3/Phd3*. Expression levels

of mRNA species were validated against an independently obtained scRNA seq data set, accessible at: <http://betsholtzlab.org/VascularSingleCells/database.html>.

### 4.4 | IF and IHC

Frozen brain sections of 15  $\mu$ m thickness were fixed in 10% neutral-buffered formalin for 30 minutes at room temperature, permeabilized with 0.5% saponin in PBS for 15 minutes, washed, and blocked in 10% normal goat serum in PBST (0.1% Tween-20 in PBS). Sections were then incubated with the respective antibodies in LowCross-Buffer<sup>®</sup> (CANDOR Biosciences, Wangen, Germany) at 4°C overnight, followed by secondary antibody incubation. ProLong<sup>®</sup> Gold Antifade Mountant with DAPI (Life Technologies, Carlsbad, CA, USA) was used for mounting. Slides were scanned with an Apiro<sup>®</sup> Versa 200 imaging system (Leica Biosystems, Richmond, IL, USA). A detailed list of antibodies used in this study can be found in Supplemental Materials and Methods (Table S2). For single (NG2) and dual (NG2/CD31) IF staining, samples were fixed in a zinc-based fixative containing 100 mmol/L Tris (pH 7.4), 3 mmol/L Calcium acetate, 25 mmol/L Zinc acetate and 35 mmol/L Zinc chloride. For quantification of the stained area, a threshold was set for background staining, and the section was analysed with NIH image analysis software ImageJ (version 1.47).

For the detection of HIF1 $\alpha$  and HIF2 $\alpha$  in formalin-fixed, paraffin-embedded brain sections an antigen retrieval solution (Agilent Dako, Santa Clara, CA, USA; #S1699) and the CSA II Biotin-free Tyramide Signal Amplification System kit (Agilent Dako, Santa Clara, CA, USA; #K1497) were used according to the manufacturer's instructions. Following overnight incubation with primary antibodies at 4°C (Table S2), sections were incubated with rabbit link (Agilent Dako, Santa Clara, CA, USA; #1501). 3,3'-Diaminobenzidine (DAB) was used as chromogenic substrate. For visualization of vascular structures IHC was combined with IF staining using lycopersicon esculentum (tomato) lectin (Vector Laboratories, Burlingame, CA, USA; #DL-1177). IHC/IF stained slides were mounted with ProLong<sup>®</sup> Gold Antifade Mountant with DAPI (Life Technologies, Carlsbad, CA, USA). Slides were scanned with an Apiro<sup>®</sup> Versa 200 imaging system (Leica Biosystems, Richmond, IL, USA) and perivascular HIF1 $\alpha$ - and HIF2 $\alpha$ -expressing cells were manually counted using the image J multipoint tool. Cell numbers were normalized by area (mm<sup>-2</sup>).

### 4.5 | RNA FISH studies

The RNA scope multiplex fluorescent kit was used for detection of *Angpt2* (488 nm) and *Pdgfrb* transcripts (750 nm)



in formalin-fixed, paraffin-embedded 10  $\mu\text{m}$  thick brain sections as per the manufacturer's protocol (Advanced Cell Diagnostics, Hayward, CA, USA). Slides were scanned with an Apero<sup>®</sup> Versa 200 imaging system (Leica Biosystems, Richmond, IL, USA). Images were captured at 40x magnification using the Leica Digital Image Hub (Leica Biosystems, Richmond, IL, USA) as previously described.<sup>14</sup>

#### 4.6 | Immunoblot analysis and gelatin zymography

Cerebral cortex and striatum were dissected on ice. Tissue was homogenized in ice-cold buffer containing 150 mmol/L NaCl, 50 mmol/L Tris-HCl, 1% NP-40, pH 8.0 supplemented with 5% protease and 1% phosphatase inhibitor cocktail (Millipore-Sigma, St. Louis, MO, USA). Protein concentrations were measured using a DC Protein Assay kit (Bio-Rad, Hercules, CA, USA). Samples were denatured in Laemmli buffer and proteins separated with 7% or 10% SDS-PAGE and transferred to PVDF membrane filters. Non-specific binding was blocked with TBS buffer containing 0.1% Tween 20 (TBST) and 5% skimmed milk (Millipore-Sigma, St. Louis, MO, USA). Membranes were incubated at 4°C overnight with antibodies detecting p-FAK (Tyr 576)-R or  $\beta$ -actin followed by incubation with secondary horseradish peroxidase-conjugated goat anti-rabbit IgG or goat anti-mouse IgG antibodies (Abcam, Cambridge, MA, USA) for 2 hours in TBST and 5% skimmed milk (Bio-Rad, Hercules, CA, USA). Immunoreactivity was detected by ECL prime enhanced chemiluminescence (Amersham, GE Healthcare, Thermo Fisher Scientific, Waltham, MA, USA).  $\beta$ -Actin was used for normalization. MMP-9 and MMP-2 activity was assessed by gelatin zymography. The same samples were subjected to SDS-PAGE electrophoresis in 9% acrylamide-bis gel containing 0.1% gelatin (Millipore-Sigma, St. Louis, MO, USA). Gels were washed, incubated for 1 hour in activation buffer (50 mmol/L Tris-HCl, 6 mmol/L  $\text{CaCl}_2$ , 1.5  $\mu\text{mol/L}$   $\text{ZnCl}_2$ , pH 7.4) containing 2.5% Triton X-100 and then incubated at 37°C for 24h in the same buffer without Triton X-100. The gels were subsequently stained with Coomassie brilliant blue R-250 (Bio-Rad, Hercules, CA, USA) followed by immersion in de-staining solution (40% methanol, 10% acetic acid, 50% water). Gels were then digitalized and densitometrically analysed with Image J (NIH image analysis software ImageJ; version 1.47).

#### 4.7 | In situ zymography

In situ gelatinolytic activity was assessed using a commercially available kit (Life Technologies, Carlsbad, CA,

USA) as previously described.<sup>69</sup> Frozen brain sections of 10  $\mu\text{m}$  thickness were incubated for 1 hour at 37°C in a humidified chamber in a reaction buffer containing the gelatin fluorescein conjugate (50  $\mu\text{g ml}^{-1}$ ). Sections were then fixed in a zinc-based fixative, washed in PBS and stained with an NG2 antibody as described earlier. ProLong<sup>®</sup> Gold Antifade Mountant with DAPI (Life Technologies, Carlsbad, CA, USA) was used for mounting and images were captured at 20x magnification using an epifluorescent microscope (Axio Imager, Carl Zeiss, Pleasanton, CA, USA).

#### 4.8 | Statistical analysis

Data are reported as mean  $\pm$  SEM. Statistical analyses were performed with Prism 5 software (GraphPad Software, Inc, La Jolla, CA, USA) using the unpaired two-tailed Student's *t* test with Welch's correction as needed, or one-way analysis of variance (ANOVA) followed by Tukey's post hoc analysis to compare between three or more groups. *P* values < .05 were considered statistically significant.

#### ACKNOWLEDGEMENTS

The data that support the findings of this study are available from the corresponding author upon reasonable request. VHH is supported by the Krick-Brooks chair in Nephrology at Vanderbilt University and was a VINNOVA Marie Curie fellow. AAU is supported by the Comunidad de Madrid and Universidad Autónoma de Madrid, grant SI1/PJI/2019-00399. NG is supported by a China Scholarship foundation grant. CMC is supported by a Spain Scholarship foundation grant. The authors would like to thank Sir Peter J. Ratcliffe and Tammy Bishop, University of Oxford, for providing the PM8 antibody and Joseph Roland from the Digital Histology Shared Resource Core at Vanderbilt University for his assistance with image analysis.

#### CONFLICT OF INTEREST

The authors declare that no conflict of interest exists.


#### AUTHOR CONTRIBUTIONS

AAU and VHH conceived and designed the research studies, analysed and interpreted data, wrote the manuscript and made the figures. AAU, NG, CMC, AA and OD performed experiments and acquired data.

#### ORCID

Andrés A. Urrutia  <https://orcid.org/0000-0001-7945-5515>

Nan Guan  <https://orcid.org/0000-0002-7156-8563>

Volker H. Haase  <https://orcid.org/0000-0002-7051-8994>

## REFERENCES

- Raichle ME, Gusnard DA. Appraising the brain's energy budget. *Proc Natl Acad Sci USA*. 2002;99(16):10237-10239.
- Girouard H, Iadecola C. Neurovascular coupling in the normal brain and in hypertension, stroke, and Alzheimer disease. *J Appl Physiol*. 2006;100(1):328-335.
- Mistry N, Mazer CD, Sled JG, et al. Red blood cell antibody-induced anemia causes differential degrees of tissue hypoxia in kidney and brain. *Am J Physiol Regul Integr Comp Physiol*. 2018;314(4):R611-R622.
- Kaelin WG, Ratcliffe PJ. Oxygen sensing by metazoans: the central role of the HIF hydroxylase pathway. *Mol Cell*. 2008;30(4):393-402.
- Semenza GL. Hypoxia-inducible factors in physiology and medicine. *Cell*. 2012;148(3):399-408.
- Ivan M, Kaelin WG. The EGLN-HIF O. *Mol Cell*. 2017;66(6):772-779.
- Berra E, Benizri E, Ginouves A, Volmat V, Roux D, Pouyssegur J. HIF prolyl-hydroxylase 2 is the key oxygen sensor setting low steady-state levels of HIF-1 $\alpha$  in normoxia. *Embo J*. 2003;22(16):4082-4090.
- Appelhoff RJ, Tian YM, Raval RR, et al. Differential function of the prolyl hydroxylases PHD1, PHD2, and PHD3 in the regulation of hypoxia-inducible factor. *J Biol Chem*. 2004;279(37):38458-38465.
- Marti HH, Wenger RH, Rivas LA, et al. Erythropoietin gene expression in human, monkey and murine brain. *Eur J Neurosci*. 1996;8(4):666-676.
- Marti HH, Risau W. Systemic hypoxia changes the organ-specific distribution of vascular endothelial growth factor and its receptors. *Proc Natl Acad Sci USA*. 1998;95(26):15809-15814.
- Boroujerdi A, Milner R. Defining the critical hypoxic threshold that promotes vascular remodeling in the brain. *Exp Neurol*. 2015;263:132-140.
- LaManna JC, Chavez JC, Pichiule P. Structural and functional adaptation to hypoxia in the rat brain. *J Exp Biol*. 2004;207(Pt 18):3163-3169.
- Bauer AT, Bürgers HF, Rabie T, Marti HH. Matrix metalloproteinase-9 mediates hypoxia-induced vascular leakage in the brain via tight junction rearrangement. *J Cereb Blood Flow Metab*. 2010;30(4):837-848.
- Urrutia AA, Afzal A, Nelson J, Davidoff O, Gross KW, Haase VH. Prolyl-4-hydroxylase 2 and 3 coregulate murine erythropoietin in brain pericytes. *Blood*. 2016;128(21):2550-2560.
- Attwell D, Mishra A, Hall CN, O'Farrell FM, Dalkara T. What is a pericyte? *J Cereb Blood Flow Metab*. 2015;36(2):451-455.
- Nishiyama A, Boshans L, Goncalves CM, Wegrzyn J, Patel KD. Lineage, fate, and fate potential of NG2-glia. *Brain Res*. 2016;1638(Pt B):116-128.
- Peppiatt CM, Howarth C, Mobbs P, Attwell D. Bidirectional control of CNS capillary diameter by pericytes. *Nature*. 2006;443(7112):700-704.
- Sweeney MD, Ayyadurai S, Zlokovic BV. Pericytes of the neurovascular unit: key functions and signaling pathways. *Nat Neurosci*. 2016;19(6):771-783.
- Minocha S, Vallotton D, Brunet I, Eichmann A, Hornung JP, Lebrand C. NG2 glia are required for vessel network formation during embryonic development. *Elife*. 2015;4:e09102.
- Armulik A, Genové G, Betsholtz C. Pericytes: developmental, physiological, and pathological perspectives, problems, and promises. *Dev Cell*. 2011;21(2):193-215.
- Hall CN, Reynell C, Gesslein B, et al. Capillary pericytes regulate cerebral blood flow in health and disease. *Nature*. 2014;508(7494):55-60.
- Hill RA, Tong L, Yuan P, Murkinati S, Gupta S, Grutzendler J. Regional blood flow in the normal and ischemic brain is controlled by arteriolar smooth muscle cell contractility and not by capillary pericytes. *Neuron*. 2015;87(1):95-110.
- Sagare AP, Bell RD, Zhao Z, et al. Pericyte loss influences Alzheimer-like neurodegeneration in mice. *Nat Commun*. 2013;4:2932.
- Ozerdem U, Grako KA, Dahlin-Huppe K, Monosov E, Stallcup WB. NG2 proteoglycan is expressed exclusively by mural cells during vascular morphogenesis. *Dev Dyn*. 2001;222(2):218-227.
- Zhu X, Bergles DE, Nishiyama A. NG2 cells generate both oligodendrocytes and gray matter astrocytes. *Development*. 2008;135(1):145-157.
- Nishiyama A, Suzuki R, Zhu X. NG2 cells (polydendrocytes) in brain physiology and repair. *Front Neurosci*. 2014;8:133.
- Kisler K, Nelson AR, Rege SV, et al. Pericyte degeneration leads to neurovascular uncoupling and limits oxygen supply to brain. *Nat Neurosci*. 2017;20(3):406-416.
- Montagne A, Nikolakopoulou AM, Zhao Z, et al. Pericyte degeneration causes white matter dysfunction in the mouse central nervous system. *Nat Med*. 2018;24(3):326-337.
- Winkler EA, Bell RD, Zlokovic BV. Pericyte-specific expression of PDGF beta receptor in mouse models with normal and deficient PDGF beta receptor signaling. *Mol Neurodegener*. 2010;5:32.
- Maisonpierre PC, Suri C, Jones PF, et al. Angiopoietin-2, a natural antagonist for Tie2 that disrupts in vivo angiogenesis. *Science*. 1997;277(5322):55-60.
- Mandriota SJ, Pepper MS. Regulation of angiopoietin-2 mRNA levels in bovine microvascular endothelial cells by cytokines and hypoxia. *Circ Res*. 1998;83(8):852-859.
- Galis ZS, Khatir JJ. Matrix metalloproteinases in vascular remodeling and atherogenesis: the good, the bad, and the ugly. *Circ Res*. 2002;90(3):251-262.
- Anagnostou A, Lee ES, Kessimian N, Levinson R, Steiner M. Erythropoietin has a mitogenic and positive chemotactic effect on endothelial cells. *Proc Natl Acad Sci USA*. 1990;87(15):5978-5982.
- Ribatti D, Presta M, Vacca A, et al. Human erythropoietin induces a pro-angiogenic phenotype in cultured endothelial cells and stimulates neovascularization in vivo. *Blood*. 1999;93(8):2627-2636.
- Arcasoy MO. The non-haematopoietic biological effects of erythropoietin. *Br J Haematol*. 2008;141(1):14-31.
- Minamishima YA, Moslehi J, Bardeesy N, Cullen D, Bronson RT, Kaelin WG Jr. Somatic inactivation of the PHD2 prolyl hydroxylase causes polycythemia and congestive heart failure. *Blood*. 2008;111(6):3236-3244.
- Armulik A, Genové G, Mäe M, et al. Pericytes regulate the blood-brain barrier. *Nature*. 2010;468(7323):557-561.
- Winkler EA, Bell RD, Zlokovic BV. Central nervous system pericytes in health and disease. *Nat Neurosci*. 2011;14(11):1398-1405.
- Lebrin F, Deckers M, Bertolino P, Ten Dijke P. TGF-beta receptor function in the endothelium. *Cardiovasc Res*. 2005;65(3):599-608.
- Yuan HT, Khankin EV, Karumanchi SA, Parikh SM. Angiopoietin 2 is a partial agonist/antagonist of Tie2 signaling in the endothelium. *Mol Cell Biol*. 2009;29(8):2011-2022.
- Eklund L, Kangas J, Saharinen P. Angiopoietin-Tie signalling in the cardiovascular and lymphatic systems. *Clin Sci (Lond)*. 2017;131(1):87-103.

42. Chu M, Li T, Shen B, et al. Angiopoietin receptor Tie2 is required for vein specification and maintenance via regulating COUP-TFII. *Elife*. 2016;5.
43. Teichert M, Milde L, Holm A, et al. Pericyte-expressed Tie2 controls angiogenesis and vessel maturation. *Nat Commun*. 2017;8:16106.
44. Yuen TJ, Silbereis JC, Griveau A, et al. Oligodendrocyte-encoded HIF function couples postnatal myelination and white matter angiogenesis. *Cell*. 2014;158(2):383-396.
45. Takeda K, Ho VC, Takeda H, Duan LJ, Nagy A, Fong GH. Placental but not heart defects are associated with elevated hypoxia-inducible factor alpha levels in mice lacking prolyl hydroxylase domain protein 2. *Mol Cell Biol*. 2006;26(22):8336-8346.
46. Minamishima YA, Kaelin WG Jr. Reactivation of hepatic EPO synthesis in mice after PHD loss. *Science*. 2010;329(5990):407.
47. Aprelikova O, Chandramouli GV, Wood M, et al. Regulation of HIF prolyl hydroxylases by hypoxia-inducible factors. *J Cell Biochem*. 2004;92(3):491-501.
48. Stiehl DP, Wirthner R, Koditz J, Spielmann P, Camenisch G, Wenger RH. Increased prolyl 4-hydroxylase domain proteins compensate for decreased oxygen levels. Evidence for an autoregulatory oxygen-sensing system. *J Biol Chem*. 2006;281(33):23482-23491.
49. Quaegebeur A, Segura I, Schmieder R, et al. Deletion or inhibition of the oxygen sensor PHD1 protects against ischemic stroke via reprogramming of neuronal metabolism. *Cell Metab*. 2016;23(2):280-291.
50. Cummins EP, Berra E, Comerford KM, et al. Prolyl hydroxylase-1 negatively regulates IkappaB kinase-beta, giving insight into hypoxia-induced NFkappaB activity. *Proc Natl Acad Sci USA*. 2006;103(48):18154-18159.
51. Cockman ME, Lippl K, Tian YM, et al. Lack of activity of recombinant HIF prolyl hydroxylases (PHDs) on reported non-HIF substrates. *Elife*. 2019;8.
52. Vanlandewijck M, He L, Mäe MA, et al. A molecular atlas of cell types and zonation in the brain vasculature. *Nature*. 2018;554(7693):475-480.
53. Zeisel A, Hochgerner H, Lönnerberg P, et al. Molecular architecture of the mouse nervous system. *Cell*. 2018;174(4):999-1014.e1022.
54. He L, Vanlandewijck M, Mäe MA, et al. Single-cell RNA sequencing of mouse brain and lung vascular and vessel-associated cell types. *Sci Data*. 2018;5:180160.
55. Asada N, Takase M, Nakamura J, et al. Dysfunction of fibroblasts of extrarenal origin underlies renal fibrosis and renal anemia in mice. *J Clin Invest*. 2011;121(10):3981-3990.
56. Simon C, Lickert H, Gotz M, Dimou L. Sox10-iCreERT2: a mouse line to inducibly trace the neural crest and oligodendrocyte lineage. *Genesis*. 2012;50(6):506-515.
57. Keith B, Johnson RS, Simon MC. HIF1alpha and HIF2alpha: sibling rivalry in hypoxic tumour growth and progression. *Nat Rev Cancer*. 2012;12(1):9-22.
58. Sandner P, Gess B, Wolf K, Kurtz A. Divergent regulation of vascular endothelial growth factor and of erythropoietin gene expression in vivo. *Pflugers Arch*. 1996;431(6):905-912.
59. Yeh TL, Leissing TM, Abboud MI, et al. Molecular and cellular mechanisms of HIF prolyl hydroxylase inhibitors in clinical trials. *Chem Sci*. 2017;8(11):7651-7668.
60. Sanghani NS, Haase VH. Hypoxia-inducible factor activators in renal anemia: current clinical experience. *Adv Chronic Kidney Dis*. 2019;26(4):253-266.
61. Wragg JW, Durant S, McGettrick HM, Sample KM, Egginton S, Bicknell R. Shear stress regulated gene expression and angiogenesis in vascular endothelium. *Microcirculation*. 2014;21(4):290-300.
62. Hardee ME, Kirkpatrick JP, Shan S, et al. Human recombinant erythropoietin (rEpo) has no effect on tumour growth or angiogenesis. *Br J Cancer*. 2005;93(12):1350-1355.
63. Lundby C, Hellsten Y, Jensen MB, Munch AS, Pilegaard H. Erythropoietin receptor in human skeletal muscle and the effects of acute and long-term injections with recombinant human erythropoietin on the skeletal muscle. *J Appl Physiol*. 2008;104(4):1154-1160.
64. Sinclair AM, Coxon A, McCaffery I, et al. Functional erythropoietin receptor is undetectable in endothelial, cardiac, neuronal, and renal cells. *Blood*. 2010;115(21):4264-4272.
65. Jelkmann W. Erythropoietin: back to basics. *Blood*. 2010;115(21):4151-4152.
66. Wang L, Zhang Z, Wang Y, Zhang R, Chopp M. Treatment of stroke with erythropoietin enhances neurogenesis and angiogenesis and improves neurological function in rats. *Stroke*. 2004;35(7):1732-1737.
67. Li Y, Lu Z, Keogh CL, Yu SP, Wei L. Erythropoietin-induced neurovascular protection, angiogenesis, and cerebral blood flow restoration after focal ischemia in mice. *J Cereb Blood Flow Metab*. 2007;27(5):1043-1054.
68. Zlokovic BV. Neurovascular pathways to neurodegeneration in Alzheimer's disease and other disorders. *Nat Rev Neurosci*. 2011;12(12):723-738.
69. Urrutia A, Rubio-Araiz A, Gutierrez-Lopez MD, et al. A study on the effect of JNK inhibitor, SP600125, on the disruption of blood-brain barrier induced by methamphetamine. *Neurobiol Dis*. 2012;50C:49-58.

## SUPPORTING INFORMATION

Additional supporting information may be found online in the Supporting Information section.

**How to cite this article:** Urrutia AA, Guan N, Mesa-Ciller C, Afzal A, Davidoff O, Haase VH. Inactivation of HIF-prolyl 4-hydroxylases 1, 2 and 3 in NG2-expressing cells induces HIF2-mediated neurovascular expansion independent of erythropoietin. *Acta Physiol*. 2021;231:e13547. <https://doi.org/10.1111/apha.13547>